JCEC
THE JOURNAL OF ENGINEERING AND EXACT SCIENCES

OPEN ACCESS

The Journal of Engineering and Exact Sciences – jCEC, Vol. 07 N. 03 (2021)
journal homepage: https://periodicos.ufv.br/ojs/jcec
ISSN: 2527-1075

Applying different techniques for evaluating the resistance to moisture of electrospun PVA nanofibers

Aplicação de diferentes técnicas de avaliação da resistência à umidade de nanofibras de PVA eletrofiadas

Article Info:
Article history: Received 2021-06-03 / Accepted 2021-08-12 / Available online 2021-08-12
doi: 10.18540/jcecvl7iss3pp12938-01-10e

Alessandro Estarque de Oliveira
ORCID: https://orcid.org/0000-0001-7900-2874
Universidade Federal de São Carlos, Brazil
E-mail: alessandroestarque@gmail.com
Mônica Lopes Aguiar
ORCID: https://orcid.org/0000-0003-4540-5776
Universidade Federal de São Carlos, Brazil
E-mail: mlaguiar@ufscar.br
Vádila Giovana Guerra
ORCID: https://orcid.org/0000-0002-0096-6329
Universidade Federal de São Carlos, Brazil
E-mail: vadila@ufscar.br

Resumo
Álcool polivinílico é utilizado para produzir nanofibras via *electrospinning* para inúmeras aplicações associadas à não-toxicidade do material. No entanto, a aplicação em filtração de ar é prejudicada devido à alta hidrofilicidade do PVA, requerendo a reticulação com aditivos. Neste trabalho, diferentes técnicas foram avaliadas para verificar a resistência à umidade de nanofibras de PVA utilizando ácido cítrico como agente reticulante. A perda de massa não revelou modificações estruturais significativas do meio filtrante devido à baixa aplicabilidade da técnica para este caso. A medida de ângulo de contato com água tampouco se mostrou adequada para as condições experimentais. Uma metodologia foi então proposta, medindo-se a queda de pressão antes e pós a passagem de ar limpo (~15.0 cm s^{-1}) contendo diferentes valores de umidade (49, 68 e 90% U.R.) para verificar a resistência das fibras ao longo do tempo (zero a 60 min). As amostras foram resistentes à umidade e mudanças estruturais significativas não ocorreram nas fibras após o procedimento, de acordo com análise de imagens de microscopia eletrônica de varredura. Para os dois menores valores de umidade, a variação da queda de pressão foi próxima a zero após 60 min, enquanto atingiu 4.1% para 90% U.R. Tal metodologia se mostrou adequada para aplicação em filtração de ar.
Palavras-chave: Nanofibras. *Electrospinning*. Hidrofilicidade.

Abstract
Poly (Vinyl Alcohol) (PVA) is used to produce nanofibers with electrospinning for several applications related to the non-toxicity of the material, however, the application in air filtration in hindered by the high hydrophilicity of the material, which requires the crosslinking with additives. In this work, different techniques were assessed to verify the moisture resistance of PVA nanofibers crosslinked with citric acid. The mass loss did not reveal significant structural modification of the filter media due to the relatively low mass of the nanofibers in comparison to the mass of the substrate, proving the poor applicability of this technique for this process. The measurement of the water contact angle was not suitable for the experimental circumstances as well. A methodology was then purposed, measuring the pressure drop before and after the flow of clean air stream (~15.0 cm s^{-1}) through the filter media with different contents of water (49, 68, and 90% R.H.) to verify the

humidity resistance of the fibers over time (zero to 60 min). The samples were resistant to humidity and no significant structural changes occurred in the fibers after the process in accordance with analysis of scanning electron microscopy images. For the two lowest humidities, variation of the pressure drop was equal to approximately zero after 60 min while it achieved 4.1% for 90% R.H. This methodology proved to be suitable for air filtration application.
Keywords: Nanofibers. Electrospinning. Hydrophilicity.

1. Introduction

Poly(vinyl alcohol) (PVA) fibers produced with the electrospinning technique are currently used in tissue scaffolds with antimicrobial activity (Esparza et al., 2017; Hong et al., 2006; Tonglairoum et al., 2015), filtration of gases (Zhu et al., 2018), and liquids effluents (Bary et al., 2018; Li; Barbari, 1995; Li; Yao, 2017), as an option to polymers that are soluble in harmful solvents such as dimethylformamide (DMF). However, PVA presents high degree of hydrophilicity due to the presence of hydroxyl groups in the polymer chains, hindering its use in the filtration of liquids and humid gases. Several methodologies are employed to preserve the structure of the spun fibers in the presence of water.

In the other hand, the nonionic surfactant Triton X-100 is used to decrease the fiber diameter and to reduce the bead formation by decreasing the surface tension of the polymer solution (Bonino et al., 2011; Du; Hsieh, 2007; Yu et al., 2012). However, the presence of the surfactant also could lead to decreasing resistance of the nanofibers in relation to humidity. Although the mass loss after immersion in water (Esparza et al., 2017; López-Córdoba et al., 2016; Lv et al., 2019; Miraftab et al., 2015; Shi; Yang, 2015; Stone et al., 2013) and water contact angle measurements (Fang et al., 2018; Lee et al., 2016) are traditionally used to evaluate the resistance to water, these methodologies seem not attesting the usefulness of the PVA filter media in air filtration, a process in which water could be present as moisture in the air stream, but there is no severe condition like immersion in pure water.

In this work, the moisture resistance of electrospun PVA nanofibers was evaluated through the techniques of mass loss after immersion in water and the water contact angle measurement. A novel methodology was purposed that assesses any structural change of the filter media after the passing through of moist air streams. This methodology includes the verification of the pressure drop of the clean filter media over time with constant passing though of air stream containing different contents of water. Scanning Electron Microscopy (SEM) images of the filter media before and after the tests are taken to evaluate any structural changes of the fibers with the moisture. This methodology could be more useful for studies concerning the reduction of the hydrophilicity of fibers for application in systems where the moisture content is moderate such as air filtration.

2. Experimental Procedure

2.1 Material

PVA (molecular weight: 104.5 kg mol^{-1}, degree of hydrolysis = 87.0–89.0 mol%) and Triton X-100 (molecular weight = 647 g mol^{-1}) were purchased from Neon (Brazil). Anhydrous citric acid (Mw = 192 g mol^{-1}) was acquired from Synth (Brazil). Cellulose filter media (PFI 25–24 RAD+, cellulose from Pinus trees, basis weight = 150 g cm^{-2}, further characterization provided below) used as a substrate for the spun fibers were kindly donated by Ahlstrom-Munksjö (Brazil).

2.2 Manufacturing and Characterization of the Fibers

PVA solution (13 wt.%) was prepared dissolving polymer pellets to deionized water with Triton X-100 (0.50 wt.%) used to obtain a more electro-spinnable solution and thin fibers (Bonino et al., 2011; Du; Hsieh, 2007; Yu et al., 2012). The mixture was agitated for 1 h, under stirring at 1150 rpm and 80ºC. Crosslinking agent citric acid (5.0 wt.% based on the PVA mass, according to

Esparza et al., 2017; López-Córdoba et al., 2016; Lv et al., 2019; Shi; Yang, 2015; Stone et al., 2013) was then added for further stirring (30 min). The solutions were then left to degas overnight. A size 500 Cannon-Fenske viscometer was used to obtain the solution viscosity. A Du-Noüy tensiometer (Model 70535, CSC) with a platinum ring was used to obtain the surface tension. A conductivity meter (Model TEC-4MP, Tecnal) was used to measure the electrical conductivity. Surface tension and electrical conductivity measurements were performed 10 times and the viscosity measurements were performed 5 times, due to the reproducibility of the results, at 25ºC. The mean values and the respective standard deviations were obtained. For the electrospinning of the fibers (Fig. 1a), the PVA solution was inserted in a syringe fitted with a needle (0.60 mm of inner diameter). The syringe was connected to an infusion pump in order to inject 0.5 mL h^{-1} of the solution over a rotating cylinder collector (10 cm diameter, rotation speed of 296 rpm) covered by the substrate. A power source provided 27 kV of voltage between the needle tip and collector, distancing 10 cm. Electrospinning was performed for 15 min. The operating conditions were established after previous tests. The humidity and temperature of the room were maintained respectively in 48% R.H. and 25ºC in average. The spun fibers were maintained in a vacuum oven at 140ºC for 2 h, following previous researches that crosslinked PVA fibers with citric acid (Esparza et al., 2017; Lv et al., 2019; Shi; Yang, 2015; Stone et al., 2013).

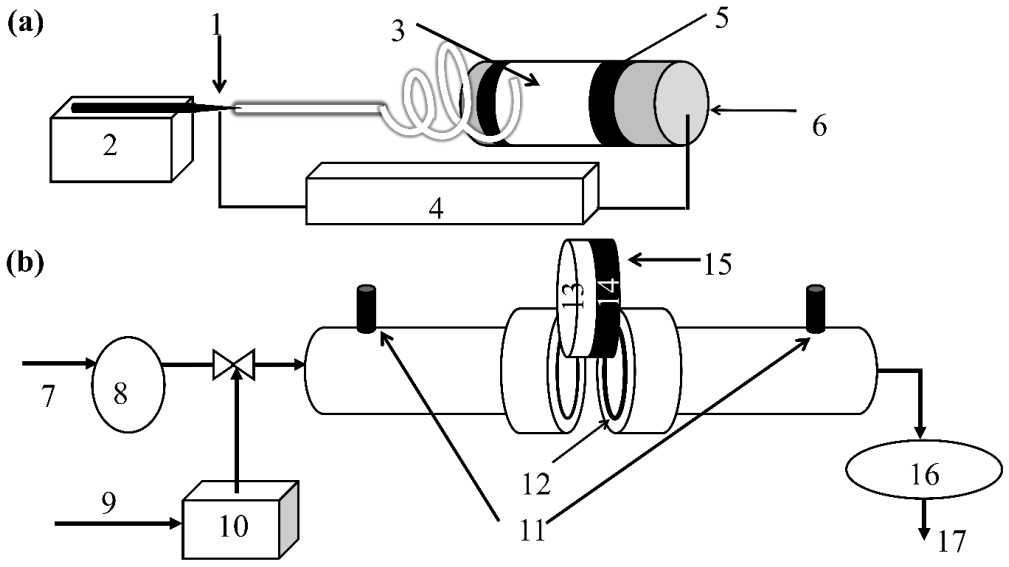

Figure 1 - Electrospinning setup (a) and experimental system of the permeability essays and moisture resistance tests (b). 1: Needle tip; 2: Infusion pump; 3: Nanofibers; 4: Power supply; 5: Substrate; 6: Rotating collector; 7: Air inlet; 8: Pre-filters; 9: Compressed air; 10: Aerosol atomizer; 11: Pressure acquisition points; 12: O-ring; 13: Nanofibers; 14: Substrate; 15: Filter medium; 16: Flowmeter; 17: Air outlet.

Fourier Transform Infrared spectroscopy (ATR-FTIR, Model Tensor 27, Bruker) was used to confirm the occurrence of crosslinking between PVA and citric acid. Samples ~2×2 cm in size cut from the cellulose substrates covered with PVA nanofibers were used. A sample of the single substrate was also sampled in order to discount the peaks related to the cellulose fibers in the spectra of the samples with PVA nanofibers.

A SEM instrument (Philips XL-30 FEG) installed in the Structural Characterization Laboratory of the Federal University of São Carlos (Brazil) was used to take images of the surface of the PVA fibers. The thicknesses of the substrate alone and the samples covered with nanofibers were analyzed using an optical microscope (Model BX60, Olympus). ImageJ software (Rasband,

2020) was used to measure the fiber diameters and the thicknesses of the samples. The methodology of measurement of the diameter from the images is described by Bortolassi et al. (2017). The diameters of 150 different fibers were measured for each sample, with calculation of the median and the Geometric Standard Deviation (GSD) of the distributions. For obtention of the thicknesses of the filter media, three images of different areas of the sample cross-section were taken with the optical microscope. The measurements were performed 15 times, obtaining the median and GSD of the distributions for each sample.

2.2 Permeability Assays and Moisture Resistance Tests

In the experimental apparatus used in the permeability essays and moisture resistance tests (Fig. 1b), atmospheric air was fed into the system from a compressor, flowing through gas pre-filters (Model 3047B, TSI) to retain impurities and humidity. An internal air compressor of the aerosol generator (Model 3079A, TSI) also fed air into a vessel containing water for the production of aerosol particles by atomization. The aerosol (droplets of deionized water in the moisture resistance tests) was mixed with the main air flow exiting the air pre-filters. The mixture passed a Kr-85 source acting as a charge neutralizer, before entering the filter holder with the filter medium (filtration area: ~5.1 cm^2, air velocity: 5.0 cm s^{-1}). Permeability tests were performed varying the air velocity (0.3–3.3 cm s^{-1}) and obtaining the respective pressure drop (ΔP) with a digital manometer (VelociCalc 9665-P, TSI) connected to pressure acquisition points distancing 12 cm from the inlet and outlet of the filter holder. The permeability constant (K) was obtained from Darcy's law:

$$\frac{\Delta P}{L} = \frac{\mu}{K} v \quad (1)$$

where v is the gas velocity [m s^{-1}], L is the thickness of the filter medium [m], and μ is the gas viscosity (1.79×10^{-5} Pa×s at 25ºC and 92 kPa (Riehle, 1997)).

The porosity of the filter medium ε [dimensionless] was obtained using the Davies equation (Davies, 1973), following works that evaluated nanofibers (Alexandrescu et al., 2016; Yang; Lee, 2005) and microfibers (Leung et al., 2010) for air filtration applications, expressed as:

$$\frac{\Delta P}{L} = \frac{v}{r^2} \times \mu \times 16 \times (1-\varepsilon)^{1.5} \times (1 + 56 \times (1-\varepsilon)^3) \quad (2)$$

where r is the fiber radius (the median value here) [m]. Parameters K and ε were obtained from the slopes of the curves of $\Delta P/L$ vs. air velocity. The results of ΔP for the single substrate were discounted from the results obtained for the association between the nanofibers and substrate in order to obtain the pressure drop exclusively due to the nanofibers (considering a series association).

In order to evaluate the resistance of the PVA nanofibers to water, three different methodologies were performed. Following previous studies (Esparza et al., 2017; López-Córdoba et al., 2016; Lv et al., 2019; Miraftab et al., 2015; Shi; Yang, 2015; Stone et al., 2013), samples of the nanofibers ~2×2 cm in size were immerged in distillated water for 24 h and then were dried in an oven at 50ºC during 2 h for drying (test A). For this case, the PVA fibers were electrospun over an aluminum foil covering the rotating collector instead of the cellulose substrate in order to avoid the influence of the cellulose fibers in the methodology due to absorption of water. The mass of the samples was measured before the immersion and after the drying in order to verify any mass loss (triplicate). The water contact angle of the samples consisting of nanofibers and substrate was also measured (test B) following previous studies (Fang et al., 2018; Lee et al., 2016) and using an Attension® tensiometer in order to verify the hydrophilicity of the PVA fibers. The tensiometer was connected to a camera that took images of a produced water droplet over the surface of the samples for each ~0.083 s starting from the drop of the droplet up to 10 s. In addition, a novel method was proposed (test C), which consisted of passing an air stream containing moisture produced by the atomization of distilled water, at a controlled flow rate, through the clean filter in the apparatus presented in Fig. 1b. By varying the flow rate of the compressed air in the aerosol generator, different flow rates of water droplets were produced for further mixing with the main air stream, subsequently different values of relative humidities were obtained. The air humidity was measured with a hygrometer connected to the air exit of the system.

The pressure drop values were acquired during 60 min, in order to evaluate the resistance of the nanofibers to the humid air stream. After the essays, the filter media were analyzed with SEM (Model Inspect S50, FEI, magnification of 10,000×, in SE mode, at 5.00 kV) to observe any structural modification in the nanofibers. There were no replicates due to the duration of this test. An air flow rate was 5.0 L min^{-1} was used, in order to provide a wet environment for the samples. Three relative humidities were evaluated: 49, 68, and 90%. The data were calculated in terms of the percentage variation of the pressure drop, in relation to the initial pressure drop: $100 \times (\Delta P - \Delta P_0)/\Delta P_0$.

3. Results and Discussion

3.1 Characterization of the Solution and the Fibers

Following the experimental procedures described before, the properties of the PVA solution were obtained: the viscosity was equal to 3.54 ± 0.03 (Pa×s), the electrical conductivity was equal to 772 ± 2 (μS cm^{-1}), and the surface tension was equal to 34.3 ± 0.4 (dyn cm^{-1}). These solution properties are associated with the electrospinnability of the fluid and therefore they are related to the size of the produced fibers and the bead formation in the fiber network (Ramakrishna et al., 2005).

Fig. 2 presents the ATR-FTIR analysis of the produced fibers. Bands at approximately 840 and 2939 cm^{-1} (backbone CH_2 symmetric stretching vibration and out-of-plane twisting) and bands at around 1080 cm^{-1} (C–O stretching) and 1415 cm^{-1} (CH_2 bending) are verified. Esterification occurred between the crosslinker and the PVA as showed by the band at around 1719 cm^{-1} associated to carboxyl and ester carbonyl C=O stretching (Esparza et al., 2017; Reddy; Yang, 2010; Shi; Yang, 2015).

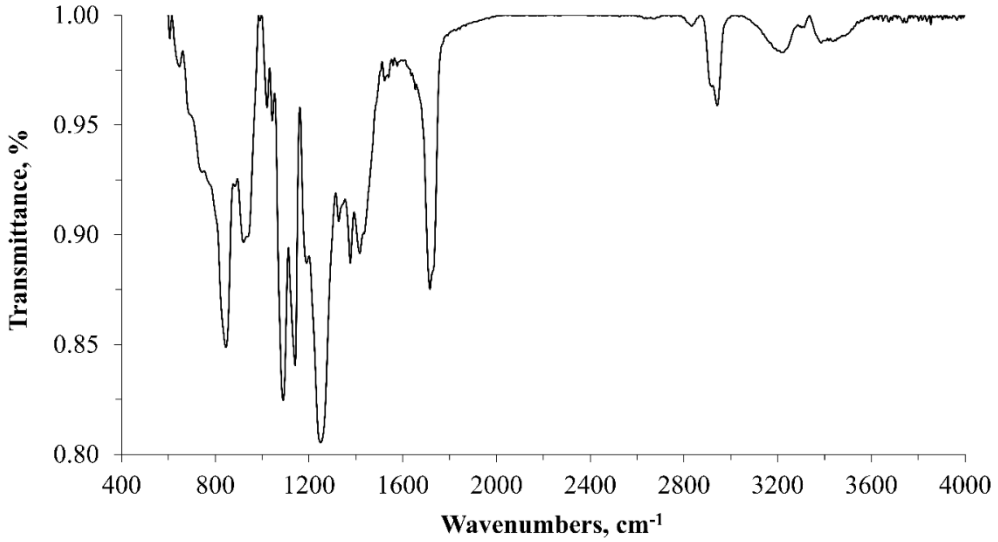

Figure 2 - ATR-FTIR analysis of the nanofiber layers.

Fig. 3 shows the particle size distribution (PSD) of the fibers of the single substrate (a) and the nanofibers layer (c), with SEM images of the microfibers (b) and the nanofibers (d), respectively. The reduction of the PSD from the substrate and the PVA fibers is noticeable and it is verified that the size range of the PVA fibers is narrower than that of the substrate, which was confirmed with the SEM image (Fig. 3 (d)) that shows homogeneous arrangement of the nanofibers mat. In Fig. 3 (d) it is possible to notice the absence of beads between the fibers. The addition of a nanofiber layer on the surface of a micro-fibrous substrate could avoid the occurrence of depth filtration since the

powder cake could be formed more quickly (Li et al., 2017). In addition, the collection of nanoparticles with diffusional mechanisms could be facilitated since the nanofiber size is smaller than the size of the microfibers, also enhancing the electrostatic attraction and reducing the distortion effect caused on the air flow by the surrounding fibers (Hinds, 1998).

The thickness of the cellulose substrate provided by the analysis of optical microscopy was 310 ± 28 (μm), while the thickness of the layer of nanofibers was 12 ± 2 (μm). The permeability tests performed as described previously (Eq. 1) provided Darcian permeability constants equal to 597×10^{-14} and 5.20×10^{-14} (m^2) respectively for the single substrate and the nanofiber layer. The porosities of the single substrate and the nanofibers layer obtained from Eq. 2 were respectively equal to 0.556 and 0.952 (dimensionless). These results mean that the nanofibers provide more resistance to the passing through of the air due to the more closed network, which in turn will require more energy consumption, even though there is too much void between the nanofibers in relation to the total volume of the nanofiber layer, as can be seen in Fig. 3 (d).

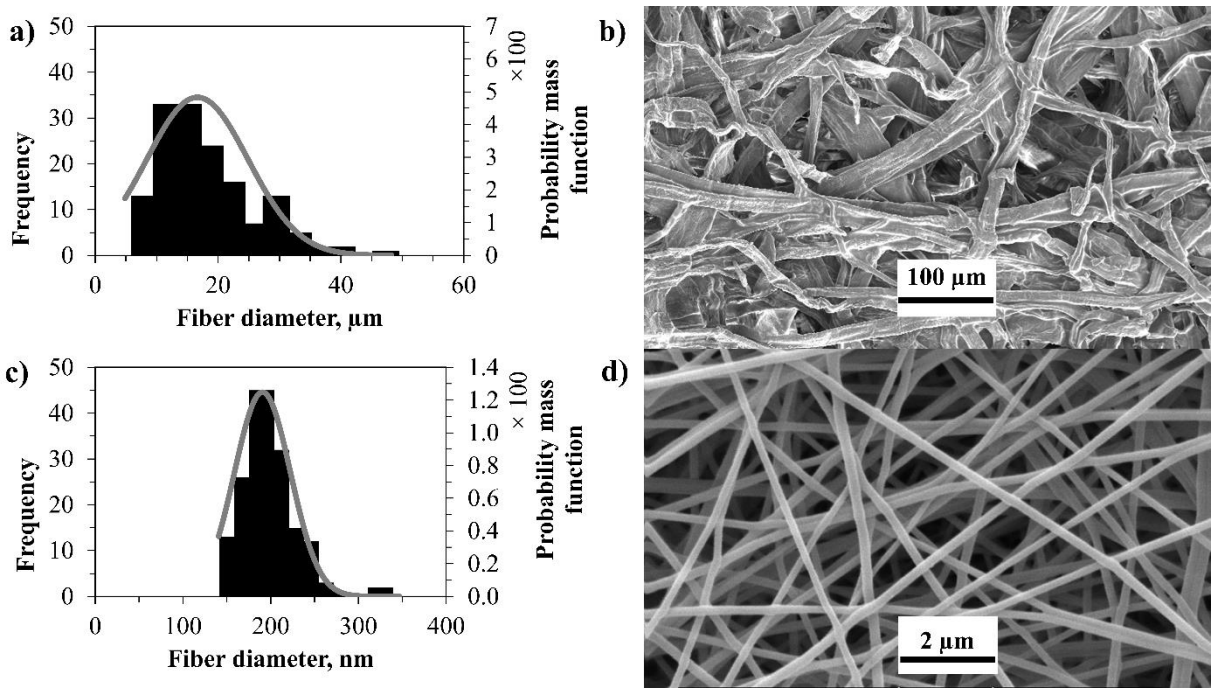

Figure 3 - PSD (a) and SEM image of the surface of the cellulosic substrate (b) (Median: 14.8 μm; GSD: 1.62); PSD (c) and SEM image of the surface of the nanofibers layer (d) (Median: 186 nm; GSD: 1.17).

3.2 Tests of Resistance to Moisture

Test A: for the production of nanofibers on the aluminum foil, the mass of the as-spun samples was 69.94 ± 0.04 (mg) and the mass after immersion in water and subsequent drying was equal to 69.51 ± 0.05 (mg), which means that the mass became 99.39% of the initial mass. In comparison with samples with no thermal crosslinking, the masses before and after immersion were 63.77 ± 0.03 and 40.53 ± 0.03 (mg), respectively. Therefore, it is verified that the PVA nanofibers were resistant to water and did not dissolve in the solvent over time when crosslinking was promoted. In fact, Miraftab et al. (2015) used this technique to evaluate nanofibers of PVA with low (LMW) and high molecular weights (HMW), treated with immersion in methanol and with heating (varying heating time from 30 min to 8 h at temperatures of 150 and 180ºC). Mass losses were measured after 24 h of immersion of fibers in water at room temperature. The authors verified no mass loss for HMW fibers treated with methanol, while different percentual mass losses were verified for LMW fibers depending on the immersion time (15 min – 24 h), varying between 9.09 (24 h) and

42.85% (30 min). For the heating treatment, no mass loss was reported for HMW fibers for all the treatment conditions, while mass loss occurred for LHW fibers depending on the time and temperature of heating, varying from zero (24 h for both temperatures) to 8.33% (1 h at 150ºC). Other results can be seen in the cited reference (Miraftab et al., 2015). However, these results do not say much about any structural changes in the fibers. In addition, this test was not performed in samples electrospun on the substrate due to the reason mentioned above, while the test with samples containing cellulosic fibers that possess greater mass than the nanofibers could hamper the results, not showing the effect of water on the PVA fibers.

Test B: Fig. 4 presents the water contact angle measurements for the droplet of distillated water over the surface of PVA nanofibers. Fig. 4 (a) exhibits the mean contact angle calculated from the left and right angles of the droplet in relation to the surface of the fibers layer, while Figs. 4 (b) and (c) are the first (after 0.083 s) and the last (after 10 s) frames captured by the camera. Due to the high hydrophilicity of the PVA nanofibers and the spider-web structure of the fibers, the droplet was rapidly absorbed by the fibers layer and then the mean contact angle decreased to zero after 2 s, from which the software of the tensiometer did not measure any angle. Zero angle also occurred in the work of Zhou et al. (2018) using polycaprolactone microfibers with polysiloxane-based surfactant and in the work of Cao et al. (2018) using PVA nanofibers with Poloxamer surfactant.

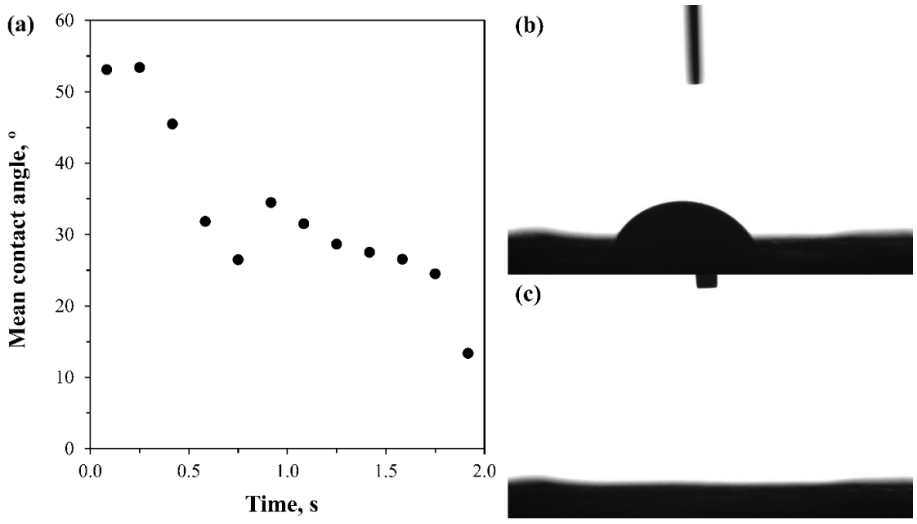

Figure 4 - Water contact angle (a) and images of the water droplet on the surface of the nanofibers layer after 0.083 s (b) and 10 s (c).

Test C: Fig. 5 presents the results obtained performing the experimental procedure described previously, with the variation of the initial pressure drop of the clean filter media over time at different air humidities (a) and SEM images of the nanofiber layer in the original state (b) and after the tests at 49% (c), 68% (d), and 90% (e) of relative humidity. It is verified in Fig. 5 (a) that the pressure drop of the filter media was kept constant over time in the experimental conditions of the test for the two lowest humidities, while there was increase of the pressure drop at the highest air humidity; this variation achieved a maximum of 4.1% of the initial pressure drop (789.1 Pa) and Fig. 5 (a) shows that this result was asymptotically achieved from approximately 35 min. This increase of the resistance to the air flow could be associated with the swelling phenomenon occurring in the PVA fibers with the presence of water, which can be visualized in the images of Fig. 5 (c) – (e). The swelling phenomenon was also reported in previous works (Lv et al., 2019; Shi; Yang, 2015; Stone et al., 2013). However, the SEM images showed that apparently no breakage of the fibers occurred with the presence of water even at the highest humidity, which could be probably verified by decreasing the resistance to the air flow over time, since there would be the appearance of holes in the fiber mat. Therefore, this methodology reveals the conditions of the fibers at different

moisture contents of air streams, being more reliable than tests A and B for applications involving gas streams, such as air filtration.

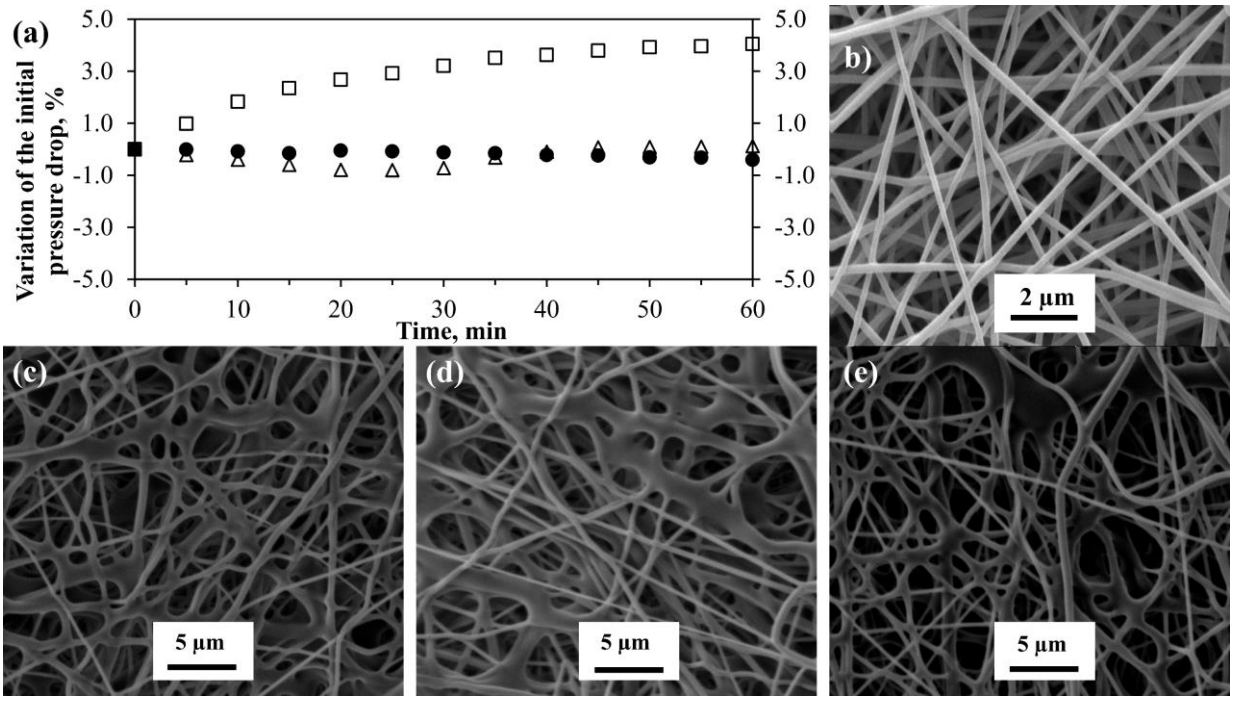

Figure 5 - Variation of the initial pressure drop over time (a) and SEM images of the nanofibers layer in the original state (b) and after 60 min of exposure of air with 49 (c), 68 (d), and 90% R.H. (e). Triangles: 49% R.H.; Spheres: 68% R.H.; Squares: 90% R.H.

4. Conclusions

The test A (mass loss) did not reveal significant structural modification of the filter media and therefore proved the poor applicability of this technique for this specific process. The measurement of the water contact angle (test B) was not suitable for the experimental circumstances as well, since the PVA presented high hydrophilicity even when crosslinked with the citric acid, as showed by the ATR-FTIR. In the methodology purposed in this work (test C), the filter media were resistant to moisture, with up to 4.1% increase of the pressure drop after 60 min of exposure to a 90% R.H. air stream and the associated SEM images showed no strong modification in the nanofibers networking despising the swelling phenomenon. The methodology purposed in the work proved to be reliable and suitable for applications where no extreme moisture environment is present, such as air filtration.

Acknowledgements

The authors are grateful for the financial support provided by CNPq (141299/2019-3) and CAPES (001). The authors also thank the Laboratory of Structural Characterization (LCE/DEMa/UFSCar) for the provision of general facilities, and Ahlstrom-Munksjö (Brazil) for supplying the cellulose filter media used in the tests.

References

Alexandrescu, L., Syverud, K., Nicosia, A., Santachiara, G., Fabrizi, A., & Belosi, F. (2016). Airborne Nanoparticles Filtration by Means of Cellulose Nanofibril Based Materials. *Journal of Biomaterials and Nanobiotechnology*, 7, 29–36. https://doi.org/10.4236/jbnb.2016.71004.

Bary, E. M. A., Fekri, A.., Soliman, Y. A., & Harmal, A. N. (2018). Characterisation and swelling–deswelling properties of superabsorbent membranes made of PVA and cellulose nanocrystals.

International Journal of Environmental Science and Technology, 76(1), 118–135. https://doi.org/10.1080/00207233.2018.1496607.

Bonino, C. A., Krebs, M. D., Saquing, C. D., Jeong, S. I., Shearer, K. L., Alsberg, E., & Khan, S. A. (2011). Electrospinning alginate-based nanofibers: From blends to crosslinked low molecular weight alginate-only systems. *Carbohydrate Polymers*, 85, 111–119. https://doi.org/10.1016/j.carbpol.2011.02.002.

Bortolassi, A. C. C., Guerra, V. G., & Aguiar, M. L. (2017). Characterization and evaluate the efficiency of different filter media in removing nanoparticles. *Separation and Purification Technology*, 175, 79–86. https://doi.org/10.1016/j.seppur.2016.11.010.

Cao, D., Li, X., Yang, L., Yan, D., Shi, Y., & Fu, Z. (2018). Controllable fabrication of micro/nanostructures by electrospinning from polystyrene/poly(vinyl alcohol) emulsion dispersions. *Journal of Applied Polymer Science*, 135, 46288. https://doi.org/10.1002/app.46288.

Davies, C. N. (1973). *Air filtration*. Academic Press.

Du, J., & Hsieh, Y. L. (2007). PEGylation of chitosan for improved solubility and fiber formation via electrospinning. *Cellulose*, 14, 543–552. https://doi.org/10.1007/s10570-007-9122-3.

Esparza, Y., Ullah, A., Boluk, Y., & Wu, J. (2017). Preparation and characterization of thermally crosslinked poly(vinyl alcohol)/feather keratin nanofiber scaffolds. *Materials Design*, 133, 1–9. https://doi.org/10.1016/j.matdes.2017.07.052.

Fang, Y., Xu, L., & Wang, M. (2018). High-Throughput Preparation of Silk Fibroin Nanofibers by Modified Bubble-Electrospinning. *Nanomaterials*, 8(7), 471. https://doi.org/10.3390/nano8070471.

Hinds, C. W. (1998). *Aerosol Technology*: Properties, Behaviour, and Measurement of Airborne Particles, 2nd edn. John Wiley.

Hong, K. W., Park, J. L., Sul, I. H., Youk, J. H., & Kang, T. J. (2006). Preparation of Antimicrobial Poly(vinyl alcohol) Nanofibers Containing Silver Nanoparticles. *Journal of Polymer Science: Polymer Physics*, 44, 2468–2474. https://doi.org/10.1002/polb.20913.

Lee, J., Boo, C., Ryu, W. H., Taylor, A. D., & Elimelech, M. (2016). Development of Omniphobic Desalination Membranes Using a Charged Electrospun Nanofiber Scaffold. *ACS Applied Materials & Interfaces*, 8, 11154–11161. https://doi.org/10.1021/acsami.6b02419.

Leung, W. W. F., Hung, C. H., & Yuen, P. T. (2010). Effect of face velocity, nanofiber packing density and thickness on filtration performance of filters with nanofibers coated on a substrate. *Separation and Purification Technology*, 71, 30–37. https://doi.org/10.1016/j.seppur.2009.10.017.

Li, M., Feng, Y., Wang, K., Yong, W. F., Yu, L., & Chung, T. S. (2017). Novel Hollow Fiber Air Filters for the Removal of Ultrafine Particles in $PM_{2.5}$ with Repetitive Usage Capability. *Environmental Science & Technology*, 51 (17), 10041–10049. https://doi.org/10.1021/acs.est.7b01494.

Li, R. H., & Barbari, T. A. (1995). Performance of poly(vinyl alcohol) thin-gel composite ultrafiltration membranes. *Journal of Membrane Science*, 105, 71–78. https://doi.org/10.1016/0376-7388(95)00048-H.

Li, Y., & Yao, S. (2017). High stability under extreme condition of the poly(vinyl alcohol) nanofibers crosslinked by glutaraldehyde in organic medium. *Polymer Degradation and Stability*, 137, 229–237. https://doi.org/10.1016/j.polymdegradstab.2017.01.018.

López-Córdoba, A., Castro, G. R., & Goyanes, S. (2016). A simple green route to obtain poly(vinyl alcohol) electrospun mats with improved water stability for use as potential carriers of drugs. *Materials Science and Engineering C*, 69, 726–732. https://doi.org/10.1016/j.msec.2016.07.058.

Lv, D., Wang, R., Tang, G., Mou, Z., Lei, J., Han, J., Smedt, S. D., Xiong, R., & Huang, C. (2019). Ecofriendly Electrospun Membranes Loaded with Visible-Light-Responding Nanoparticles for Multifunctional Usages: Highly Efficient Air Filtration, Dye Scavenging, and Bactericidal

Activity. *ACS Applied Materials & Interfaces*, 11, 12880–12889. https://doi.org/10.1021/acsami.9b01508.

Miraftab, M., Saifullah, A. N., & Çay, A. (2015). Physical stabilisation of electrospun poly(vinyl alcohol) nanofibres: comparative study on methanol and heat-based crosslinking. *Journal of Materials Science*, 50,1943–1957. https://doi.org/10.1007/s10853-014-8759-1.

Ramakrishna, S., Fujihara, K., Teo, W. E., Lim, T. C., & Ma, Z. (2005). *An Introduction of Electrospinning and Nanofibers*. World Scientific Publishing.

Rasband, W. S. (2020). *ImageJ*, U. S. National Institutes of Health, Bethesda, Maryland, USA, https://imagej.nih.gov/ij/, 1997-2021.

Reddy, N., & Yang, Y. (2010). Citric acid cross-linking of starch films. *Food Chemistry*, 118, 702–711. https://doi.org/10.1016/j.foodchem.2009.05.050.

Riehle, C. (1997). Electrostatic precipitation. In: Seville, J. P. K. (ed). *Gas cleaning in demanding applications*. Blackie Academic & Professional, pp. 193–228.

Shi, J., & Yang, E. (2015). Green electrospinning and crosslinking of polyvinyl alcohol/ citric acid. *Journal of Nanoparticle Research*, 32, 32–42. https://doi.org/10.4028/www.scientific.net/JNanoR.32.32.

Stone, S. A., Gosavi, P., Athauda, T. J., & Ozer, R. R. (2013). In situ citric acid crosslinking of alginate/polyvinyl alcohol electrospun nanofibers. *Materials Letters*, 112, 32–35. https://doi.org/10.1016/j.matlet.2013.08.100.

Tonglairoum, P., Ngawhirunpat, T., Rojanarata, T., Kaomongkolgit, R., & Opanasopit, P. (2015). Fabrication of a novel scaffold of clotrimazole-microemulsion-containing nanofibers using an electrospinning process for oral candidiasis applications. *Colloids and Surfaces B: Biointerfaces*, 126, 18–25. https://doi.org/10.1016/j.colsurfb.2014.12.009.

Yang, S., & Lee, G. W. M. (2005). Filtration characteristics of a fibrous filter pretreated with anionic surfactants for monodisperse solid aerosols. *Journal of Aerosol Science*, 36, 419–437. https://doi.org/10.1016/j.jaerosci.2004.10.002.

Yu, D. G., Chatterton, N. P., Yang, J. H., Wang, X., & Liao, Y. Z. (2012). Coaxial Electrospinning with Triton X-100 Solutions as Sheath Fluids for Preparing PAN Nanofibers. *Macromolecular Materials and Engineering*, 297, 395–401. https://doi.org/10.1002/mame.201100258395.

Zhou, F. L., Li, Z., Gough, J. E., Cristinacce, P. L. H., & Parker, G. J. M. (2018). Axon mimicking hydrophilic hollow polycaprolactone microfibres for diffusion magnetic resonance imaging. *Materials & Design*, 137, 394–403. https://doi.org/10.1016/j.matdes.2017.10.047.

Zhu, M., Hua, D., Pan, H., Wang, F., Manshian, B., Soenen, S. J., Xiong, R., & Huang, C. (2018). Green electrospun and crosslinked poly(vinyl alcohol)/poly(acrylic acid) composite membranes for antibacterial effective air filtration. *Journal of Colloid and Interface Science*, 511, 411–423. https://doi.org/10.1016/j.jcis.2017.09.101.